RELIABILITY ANALYSIS OF A THAP MISSION WITH SEQUENTIAL PHASES

Rasmi K[a], Dharmaraja Selvamuthu[a], Raina Raj[b],
Vladmir Vishnevsky[c], Dimitry Kozyrev[d]

•

Department of Mathematics, Indian Institute of Technology Delhi, New Delhi, India[a]
rasmikcnair@gmail.com
dharmar@maths.iitd.ac.in
Bharti School of Telecommunication Technology & Management,
Indian Institute of Technology Delhi, New Delhi, India[b]
rainaraj.curaj@gmail.com
V.A. Trapeznikov Institute of Control Sciences of Russian Academy of Sciences, Russia[c]
vishnevsky@ipiran.ru
RUDN University, 6 Miklukho-Maklaya St, Russian Federation[d]
kozyrev@ipiran.ru

Abstract

Stratospheric platforms, commonly known as high-altitude platforms (HAPs), are gaining traction as an economical and sustainable option for diverse applications, including environmental monitoring, surveillance, and communication networks. Tethered HAPs (tHAPs), which remain physically connected to the ground, provide improved stability, a continuous power source, and dependable data transfer capabilities. Analyzing the reliability of these systems as phased mission systems (PMS) is essential, given the multiple operational stages they undergo-such as ascend, primary task, and descend, posing distinct operational demands and challenging environmental conditions. Maintaining reliability throughout these phases is crucial for ensuring both mission effectiveness and long-term operational integrity. This research explores the necessity and practicality of conducting reliability assessments on tethered HAP systems by modeling them as PMS with well-defined stages. A comprehensive evaluation is performed for each phase, accounting for potential risks and operational constraints. Furthermore, a numerical example illustrates the reliability assessment methodology, incorporating Markovian techniques to derive key performance indicators and reliability measures for every phase.

Keywords: tHAPs, PMS, Recoverable failures, state-space based approach, Reliability.

1. Introduction

High-altitude platforms (HAPs) are aerial stations positioned between 15 and 50 kilometers above Earth's surface, maintaining a relatively fixed location. Tethered high-altitude platforms (tHAPs) enable prolonged operation by remaining anchored to the ground via a tether, usually positioned at an altitude of 100-150 meters. These platforms receive power through copper cables linked to ground-based energy sources, which sustain both their propulsion systems and onboard equipment. When compared to traditional aircraft and balloons, tHAPs offer significant advantages in terms of affordability, deployment efficiency, upkeep, mobility, and overall operational feasibility.

DOI: https://doi.org/10.24412/1932-2321-2025-489-69-81

The development of next generation tHAP systems utilizing unmanned aerial vehicles (UAVs) is actively progressing across the globe. Vishnevsky et al. [10] provide insights into the structural design, system architecture, and technological hurdles of tethered HAPs, drawing from ICS RAS™s expertise in their development and deployment. The study in [11] presents an optimized high voltage conducting tether design that enhances power transmission from ground sources, offering techniques to evaluate wave impedance and determine the required cable configuration. A Markovian framework for power management in lithium-ion battery-supported wireless communication is introduced in [15], accounting for fluctuations in energy demand as battery levels deplete. Strategies for standardization and system unification to improve operational efficiency are explored in [9]. Reliability assessments employing multidimensional and semi-Markov models for failure analysis in tHAPs are discussed in [8, 13]. Additionally, [12] examines key design considerations for advanced tHAP-based telecommunications infrastructure, emphasizing autonomous high-altitude operations, improved navigation precision, and the application of high-frequency resonance-based power transfer techniques.

Due to the absence of comprehensive monographs on the subject, [17] was developed to explore various k-out-of-n models, analytical methodologies, and their applications in assessing the reliability of tethered high-altitude telecommunication systems. One particular application of these models is discussed in [1], where the k-out-of-n: F model was utilized to evaluate the reliability of a flying module within a tethered high-altitude telecommunication platform. An analytical approach for the k-out-of-n: G model under two distinct failure scenarios was introduced in [2]. Additionally, [3] proposed a k-out-of-n system incorporating repair in a hot standby configuration. The study in [4] highlights the crucial role of the tether, composed of multiple parallel wires, in determining the overall reliability of tHAP systems.

tHAP systems function across multiple operational phases, each involving distinct tasks, environmental conditions, and success criteria. Stages such as launch, cruise, and retrieval introduce specific challenges and potential failure risks. Phased Mission Systems (PMSs) progress through successive phases, where each stage has unique performance requirements, and failures in earlier phases can influence subsequent ones. This highlights the critical importance of reliability analysis for complex systems. The interest in studying tHAP systems as phased mission systems (PMSs) is driven by [22], which offers an extensive review of advancements in PMS reliability evaluation and optimization. However, there is still a lack of research applying phased mission modeling to assess the reliability of tHAP systems.

Analytical modeling and simulations serve as essential tools for evaluating the reliability of tHAP systems. In non-repairable PMS, a failure in any phase can lead to mission termination, as in-mission repairs are not feasible [26, 23]. Conversely, repairable PMSs allow certain components to be repaired or replaced, enhancing system resilience [19, 18, 24, 25]. Failures in these systems may occur independently or result from common cause failures (CCFs), where multiple components are affected by a single underlying factor [5, 6, 7]. Additionally, functional dependence (FDEP) introduces further complexity, as the failure of one component can trigger the malfunction of others [21].

The paper is structured as follows. Section 2 describes the system componets and the nature of the mission. Section 3 includes state-space-oriented reliability analysis for tHAP systems, followed by numerical illustrations in Section 4. Finally, Section 5 provides the conclusion and future works.

2. System Description

The performance of a tHAP system relies on the integrity of its key components. A power source failure leads to a total system shutdown, disabling the rotors, communication, camera, and tether control, ultimately resulting in failure across all phases. Loss of communication isolates the HAP, preventing control, data transmission, and real-time monitoring, which directly impacts navigation and surveillance. If a rotor malfunctions during deployment, altitude control is lost, disrupting the launch sequence. In the operational phase, a camera failure hampers monitoring,

reducing mission effectiveness. A tether failure can destabilize or completely detach the HAP, jeopardizing both launch and operational phases, and potentially leading to loss of control or a crash. The impact of these failures varies by phase, but each poses a significant risk to overall mission success.

A tHAP system consists of an aerial platform linked to a Ground Control Station (GCS) via a tether, which facilitates both power and data transmission. Figure 1 illustrates this architecture, where onboard sensors and ground-based anchors monitor navigation parameters, while stabilization circuits dynamically adjust the platform™s position. Power is supplied from a ground-based source, and a smart winch mechanism controls the tether™s length to ensure optimal operation.

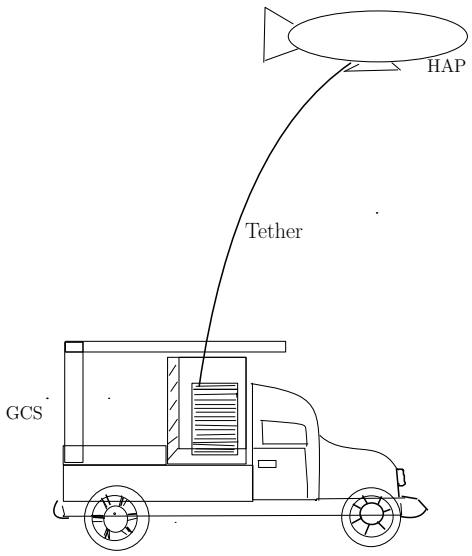

Figure 1: *A tHAP system with its major components*

A tHAP system is a specialized form of high-altitude platform that stays physically linked to the ground through a tether, serving purposes such as stability, power delivery, and data transmission. When analyzed as a phased mission system (PMS), its operation is divided into sequential phases, each demanding specific strategies for mission success. The system's operational reliability hinges on three key phases: launch, operational, and retrieval, all of which are sustained by critical components, including the Ground Control Station (GCS), the tether, and the aerial subsystem. While failures in the GCS and aerial subsystem can often be addressed through recovery mechanisms, any malfunction of the tether is considered irrecoverable. This is crucial because the tether not only ensures the physical connection and stability of the aerial subsystem but also facilitates power and data transmission. A failure in the tether could lead to severe consequences, compromising the system™s overall functionality and safety.

A tHAP System Mission phases can be classified as follows:

1. Ascend(Phase 1): The HAP is deployed and ascends to its designated operational altitude. Managing tether tension and length, ensuring smooth ascent without entanglement, and addressing environmental factors such as wind and weather conditions.

2. Primary task(Phase 2): The HAP performs its primary mission, which may involve surveillance, communication relay, or environmental monitoring. Maintaining uninterrupted power and data transmission via the tether, managing onboard payloads, and dynamically adjusting to environmental or mission-related changes.

3. Descend (Phase 3): The HAP is safely brought back to the ground. Ensuring a controlled descent, preventing tether entanglement or structural damage, and achieving a safe landing while preserving both the platform and the tether.

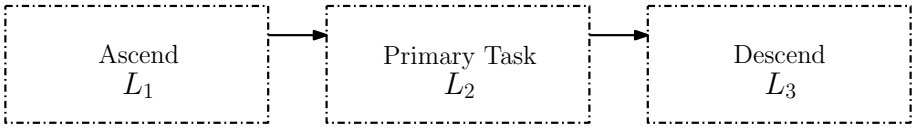

Figure 2: *Phases of a tHAP system*

3. Reliability Analysis Using CTMC Model

The reliability of a tHAP system, structured as a PMS, could be analyzed using a Continuous-Time Markov Chain (CTMC). This method characterizes system states, encompassing operational phases, failures, and repairs, with transitions governed by failure and repair rates. Distinct mission phases impose specific conditions that affect state transitions. The CTMC framework models the failure behavior of essential components such as the tether, communication modules, and power units. By leveraging state-transition matrices, it evaluates both steady-state and transient reliability measures, pinpointing critical phases and informing design enhancements and maintenance strategies.

The system is composed of three essential components and operates through three distinct mission phases. Phase transitions are assumed to be instantaneous, and all subsystems begin in an optimal state. The key components include the Ground Control Station (GCS) (C_1), the tether (C_2), and the aerial unit (C_3). Each of these components plays a vital role, with their significance and susceptibility varying across different mission phases. Failures could be distinguished as follows:

- Type I : Recoverable through repairs, does not cause mission failure.
- Type II : Unrecoverable, leading to mission failure.

Each component can exist in one of three states:

- 2: Operational
- 1: Recoverable (with Type I failure)
- 0: Failed (with Type II failure)

Components C_1 (GCS) and C_3 (aerial unit) can exist in any of three possible states, whereas component C_2 (tether) has only two states: functional (2) or failed (1). Repairs, when feasible, can be conducted while the system remains operational, and upon completion, each repaired component is restored to an "as good as new" condition. The fault tree representation of the system is illustrated in Figure 3. Here, C_j^m represents the state of component j, where $j \in \{1, 2, 3\}$ and $m \in \{0, 1, 2\}$.

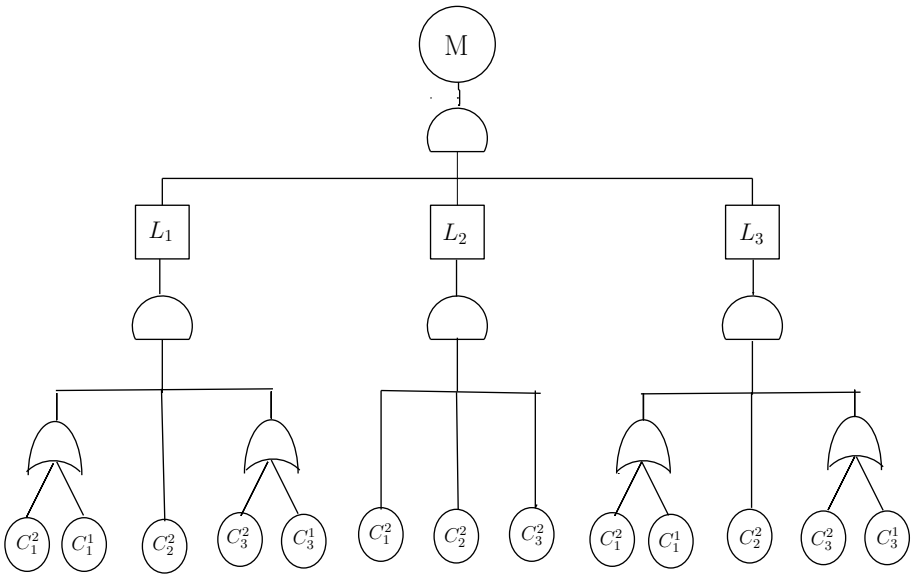

Figure 3: *Fault tree representation of the tHAP Mission*

The system's state at any given time t , where $0 \leq t \leq T$, is expressed as $(C_1(t), C_2(t), C_3(t))$. Here, $C_1(t)$ and $C_3(t)$ can assume values from $\{0, 1, 2\}$, whereas $C_2(t)$ is restricted to two states: 2 (Operational) or 0 (failed). As the workload of each subsystem may shift between phases, failure and repair rates are subject to variation. The system can exist in the following possible states:

Table 1: *List of possible states for the underlying stochastic process*

Perfect	**Faulty but operational**	**Failure**
$S_1 = (2,2,2)$	$S_2 = (1,2,2)$	$S_5 = (1,0,2)$
	$S_3 = (2,2,1)$	$S_6 = (1,2,0)$
	$S_4 = (1,2,1)$	$S_7 = (0,2,2)$
		$S_8 = (2,0,2)$
		$S_9 = (2,2,0)$
		$S_{10} = (0,2,1)$
		$S_{11} = (2,0,1)$
		$S_{12} = (1,0,1)$

The possible state transitions remain consistent across all phases, as shown in Figure 4. The mission comprises three consecutive phases, each defined by distinct success conditions. Phase L_1 always initiates with the system in state S_1. For this phase to be deemed successful, it must end in one of the states S_1, S_2, S_3, or S_4. Subsequently, Phase L_2 starts from the final successful state of Phase L_1. To ensure a smooth transition to Phase L_3, Phase L_2 should ideally end in state S_1. Since Phase L_2 serves as the primary operational phase, where the main task is executed, all type I faults must be cleared, and all subsystems must be fully functional before its completion. If Phase L_2 ends in S_2, S_3, or S_4, the system can still transition to Phase L_3, but the mission will be classified as a failure. In Phase L_3, mission success is determined by completing the phase, even if minor recoverable errors remain. This indicates that the system retains sufficient reliability to achieve overall mission success despite minor issues.

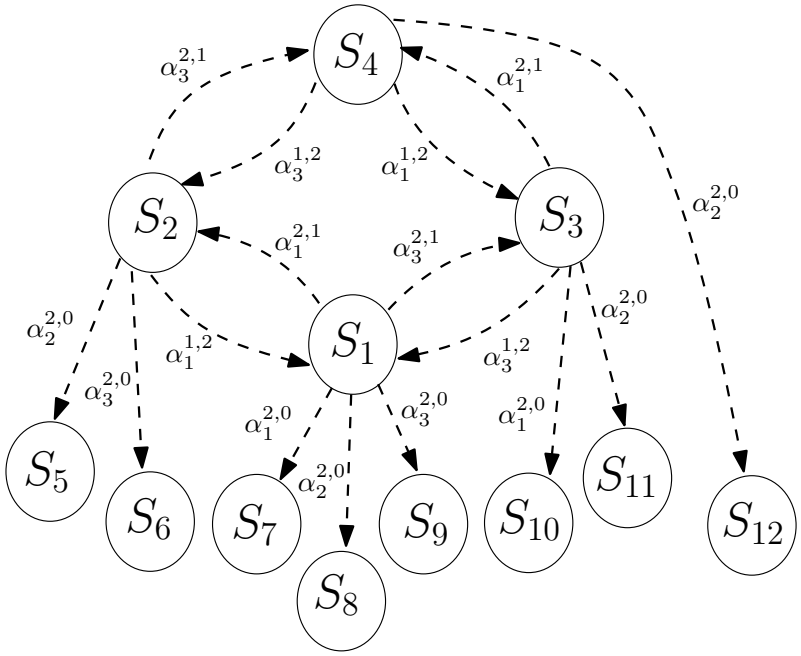

Figure 4: *State transition diagram for the underlying CTMC*

Table 2: *Initial and final states for the phases*

	Phase L_1	Phase L_2	Phase L_3
Initial states	S_1	S_1, S_2, S_3, S_4	S_1
Final states indicating phase success	S_1, S_2, S_3, S_4	S_1	S_1, S_2, S_3, S_4

When analyzing the reliability of tHAP systems as a phased mission system (PMS) where the system undergoes different operational phases with distinct reliability requirements and configurations, the Markov approach, particularly the use of CTMC, proves to be highly effective. This method captures system deterioration, repair processes, and transitions between operational modes across different phases. By specifying failure and repair rates for each component and phase, the CTMC framework enables the computation of system survival probabilities.

Each component is assumed to fail according to an exponential distribution, implying that component failure rates remain constant over time. The failure and repair rates of the components are treated as independent random variables, both governed by an exponential distribution. For component C_j, the transition rate from state m to state n is denoted as $\alpha_j^{m,n}$, where $j \in \{1, 2, 3\}$ and $m, n \in \{0, 1, 2\}$. It is important to note that a component's failure rate may vary across different phases due to fluctuations in workload and operational demands.

The state of the system at any time t during a Phase L_i is given by the process

$$\{(C_1^i(t), C_2^i(t), C_3^i(t), T_1 + ... + T_{i-1} \leq t \leq T_1 + ... + T_i\}$$

, where each $C_j^i(t)$ denotes the level of component C_j and takes values in $\{0, 1, 2\}$ depending on the assumptions for the components in respective phases. The infinitesimal generator matrix for the CTMC in each Phase L_i is denoted by $\mathbf{Q_i}$.

3.0.1 Phase L_1:

The mission is structured into three phases, each lasting T_1, T_2, and T_3 hours, respectively, with a total duration of T hours. It begins with Phase L_1, where all three components are fully operational. The initial state probabilities for Phase L_1 are given by $[1, 0, \ldots, 0]$.

The state equations governing the Markov model follow the forward Kolmogorov equation, expressed in matrix form as:

$$\mathbf{q_1}'(t) = \mathbf{q_1}(t).\mathbf{Q_1} \tag{1}$$

where $\mathbf{q_1}(t) = (q_1^1(t), q_2^1(t), \ldots, q_{12}^1(t))$ represents the state probability vector in Phase L_1. Specifically, $q_k^1(t)$, for $k \in \{1, 2, \ldots, 12\}$, denotes the probability of the system being in state S_k at any time $t \in [0, T_1]$. The term $\mathbf{q_1}'(t)$ represents the time derivative of $\mathbf{q_1}(t)$. The matrix $\mathbf{Q_1}$ is the infinitesimal generator matrix, which defines the transition rates between states in Phase L_1, as illustrated in Figure 4.

$$\mathbf{Q_1} = \begin{bmatrix} X_1 & X_2 \\ \mathbf{0} & \mathbf{0} \end{bmatrix}$$

where $\mathbf{X_1}$ contains the transition rates among the transient states, while $\mathbf{X_2}$ represents the transition rates to the absorbing states. The remaining two blocks are zero matrices of appropriate dimensions, indicating that no transitions occur from the absorbing states.

$$\mathbf{X_1} = \begin{pmatrix} a_1 & \alpha_{1,1}^{2,1} & \alpha_{1,3}^{2,1} & 0 \\ \alpha_{1,1}^{1,2} & b_1 & 0 & \alpha_{1,3}^{2,1} \\ \alpha_{1,3}^{1,2} & 0 & c_1 & \alpha_{1,1}^{2,1} \\ 0 & \alpha_{1,3}^{1,2} & \alpha_{1,1}^{1,2} & d_1 \end{pmatrix}_{4\times 4}$$

$$\mathbf{X_2} = \begin{pmatrix} 0 & 0 & \alpha_{1,1}^{2,0} & \alpha_{1,2}^{2,0} & \alpha_{1,3}^{2,0} & 0 & 0 & 0 \\ \alpha_{1,2}^{2,0} & \alpha_{1,3}^{2,0} & 0 & 0 & 0 & 0 & 0 & 0 \\ 0 & 0 & 0 & 0 & 0 & \alpha_{1,1}^{2,0} & \alpha_{1,2}^{2,0} & 0 \\ 0 & 0 & 0 & 0 & 0 & 0 & 0 & \alpha_{1,2}^{2,0} \end{pmatrix}_{4\times 8}$$

Note that the entries a_1, b_1, c_1 and d_1 of the matrix $\mathbf{X_1}$ are such that each row sum is zero.

To compute the state probability vector $\mathbf{q_1}(t)$, the system of differential equations in (1) is solved using the initial state probabilities $[1, 0, \ldots, 0]$. The state probabilities at the end of Phase L_1 (i.e., at mission time T_1 hours) are given by $(q_1^1(T_1), q_2^1(T_1), \ldots, q_{12}^1(T_1))$. With these probabilities, all reliability metrics of the multi-state system can be effectively determined. The system is considered reliable at the conclusion of Phase L_1 if it resides in any of the states S_1, S_2, S_3 or S_4. Consequently, the system reliability at the end of Phase L_1 , represented as $R_{L_1}(T_1)$, is given by

$$R_{L_1}(T_1) = q_1^1(T_1) + q_2^1(T_1) + q_3^1(T_1) + q_4^1(T_1). \tag{2}$$

3.0.2 Phase L_2:

In a multi-phase system, the transition between phases is governed by the final-state occupation probabilities of the preceding phase, which act as the initial-state probabilities for the next. As Phase L_2 begins, the system is in one of the states S_1, S_2, or S_3. To construct the Markov chain for Phase L_2, only the relevant state transitions for this phase are considered. Utilizing the final-state probabilities of Phase L_1, i.e., $(q_1^1(T_1), q_2^1(T_1), \ldots, q_{12}^1(T_1))$, to establish the initial probabilities, the equation is given by

$$\mathbf{q_2}'(t) = \mathbf{q_2}(t).\mathbf{Q_2} \tag{3}$$

for Phase L_2 is computed, yielding the system state probability vector $\mathbf{q_2}(t) = (q_1^2(t), q_2^2(t), \ldots q_{12}^2(t))$ incorporating the state probabilities $q_k^1(t), k \in \{1, 2, \ldots, 12\}$ in time $[T_1, T_1 + T_2]$.

$$\mathbf{Q_2} = \begin{bmatrix} \mathbf{Y_1} & \mathbf{Y_2} \\ \mathbf{0_1} & \mathbf{0_2} \end{bmatrix}$$

$$\mathbf{Y_1} = \begin{pmatrix} a_2 & \alpha_{2,1}^{2,1} & \alpha_{2,3}^{2,1} & 0 \\ \alpha_{2,1}^{1,2} & b_2 & 0 & \alpha_{2,3}^{2,1} \\ \alpha_{2,3}^{1,2} & 0 & c_2 & \alpha_{2,1}^{2,1} \\ 0 & \alpha_{2,3}^{1,2} & \alpha_{2,1}^{1,2} & d_2 \end{pmatrix}$$

$$\mathbf{Y_2} = \begin{pmatrix} 0 & 0 & \alpha_{2,1}^{2,0} & \alpha_{2,2}^{2,0} & \alpha_{2,3}^{2,0} & 0 & 0 & 0 \\ \alpha_{2,2}^{2,0} & \alpha_{2,3}^{2,0} & 0 & 0 & 0 & 0 & 0 & 0 \\ 0 & 0 & 0 & 0 & 0 & \alpha_{2,1}^{2,0} & \alpha_{2,2}^{2,0} & 0 \\ 0 & 0 & 0 & 0 & 0 & 0 & 0 & \alpha_{2,2}^{2,0} \end{pmatrix}_{4\times 8}$$

Note that the entries a_2, b_2, c_2 and d_2 of the matrix $\mathbf{Y_1}$ are such that each row sum is zero.

Upon completing Phase L_2 of duration T_2, the state probabilities $\mathbf{q_2}(T_1+T_2) = (q_1^2(T_1+T_2), q_2^2(T_1+T_2), \ldots, q_{12}^2(T_1+T_2))$ are calculated. Based on these state probabilities, the system reliability, represented as $R_{L_2}(T_1+T_2)$, is given by

$$R_{L_2}(T_1+T_2) = q_1^2(T_1+T_2). \tag{4}$$

3.0.3 Phase L_3:

As the mission advances to Phase L_3, its duration is represented as T_3, while the overall mission duration is given by $T\ (= T_1+T_2+T_3)$. The initial state probability vector for Phase L_3 is derived from the final state probability vector of Phase L_2, i.e., $\mathbf{q_2}(T_1+T_2)$. Using $\mathbf{q_2}(T_1+T_2)$, the equation is solved to compute the probabilities of various system states.

$$\mathbf{q_3}'(t) = \mathbf{q_3}(t).\mathbf{Q_3} \tag{5}$$

to obtain state probability vector, $\mathbf{q_3}(t) = (q_1^3(t), q_2^3(t), \ldots q_{12}^3(t)), T_1+T_2 \le t \le T$, for Phase L_3.

$$\mathbf{Q_3} = \begin{bmatrix} \mathbf{Z_1} & \mathbf{Z_2} \\ \mathbf{0_1} & \mathbf{0_2} \end{bmatrix}$$

$$\mathbf{Z_1} = \begin{pmatrix} a_3 & \alpha_{3,1}^{2,1} & \alpha_{3,3}^{2,1} & 0 \\ \alpha_{3,1}^{1,2} & b_3 & 0 & \alpha_{3,3}^{2,1} \\ \alpha_{3,3}^{1,2} & 0 & c_3 & \alpha_{3,1}^{2,1} \\ 0 & \alpha_{3,3}^{1,2} & \alpha_{3,1}^{1,2} & d_3 \end{pmatrix}$$

$$\mathbf{Z_2} = \begin{pmatrix} 0 & 0 & \alpha_{3,1}^{2,0} & \alpha_{3,2}^{2,0} & \alpha_{3,3}^{2,0} & 0 & 0 & 0 \\ \alpha_{3,2}^{2,0} & \alpha_{3,3}^{2,0} & 0 & 0 & 0 & 0 & 0 & 0 \\ 0 & 0 & 0 & 0 & 0 & \alpha_{3,1}^{2,0} & \alpha_{3,2}^{2,0} & 0 \\ 0 & 0 & 0 & 0 & 0 & 0 & 0 & \alpha_{3,2}^{2,0} \end{pmatrix}_{4\times 8}$$

Note that the entries a_3, b_3, c_3 and d_3 of the matrix $\mathbf{Z_1}$ are such that each row sum is zero.

During Phase L_3, the probability of the system being in each possible state at any time $t \in [T_1+T_2, T]$ is represented by the state probabilities $(q_1^3(t), q_2^3(t), \ldots, q_{12}^3(t))$. At the end of Phase L_3, the system's reliability, represented as $R_{L_3}(T)$, corresponds to the total system reliability, $R_{\text{sys}}(T)$. This value is derived from the state probabilities and is expressed as

$$R_{\text{sys}}(T) = R_{L_3}(T) = q_1^3(T) + q_2^3(T) + q_3^3(T) + q_4^3(T). \tag{6}$$

4. Numerical Illustrations

A numerical evaluation of the reliability of a tHAP system, modeled as a PMS, is conducted in this section. Each phase of the mission introduces distinct operational requirements and reliability challenges due to varying environmental conditions and performance criteria. The numerical illustration of the tHAP system using CTMC provides a comprehensive framework for analyzing its reliability. The CTMC model facilitates the examination of system state transitions under the assumption of exponentially distributed sojourn times.

The mission is assumed to be completed in 24hrs, where Phase L_1 takes 3hrs, Phase L_2 is planned for 19hrs, and Phase L_3 may take 2hrs, .i.e., $T = 24, T_1 = 3, T_2 = 19$, and $T_3 = 2$.

4.1. CTMC Approach

The failure and repair rates of each component in each Phase have been assumed as follows:

Table 3: *Transition rates for different phases*

	$\alpha_1^{1,2}$	$\alpha_3^{1,2}$	$\alpha_1^{2,1}$	$\alpha_3^{2,1}$	$\alpha_1^{2,0}$	$\alpha_2^{2,0}$	$\alpha_3^{2,0}$
$\mathbf{L_1}$	0.3	0.4	0.07	0.08	0.02	0.01	0.01
$\mathbf{L_2}$	0.5	0.6	0.06	0.05	0.006	0.006	0.007
$\mathbf{L_3}$	0.3	0.3	0.07	0.08	0.02	0.02	0.02

4.1.1 Phase L_1

As the state transitions diagram 4, and Table 1 indicates, the system initiates functioning in Phase L_1 with the probability vector $[1, 0, \ldots, 0]$ at time $t = 0$. Solving (1) for Phase L_1, the probability vector $\mathbf{q_1}(t)$ is obtained which describes the system as well as the components' state during the time span $[0, 3]$. The reliability curves are plotted to understand the effect of failure rates of the components, GCS($\alpha_{1,1}^{2,0}$), tether($\alpha_{1,2}^{2,0}$), and AS($\alpha_{1,3}^{2,0}$) in Figure 5.

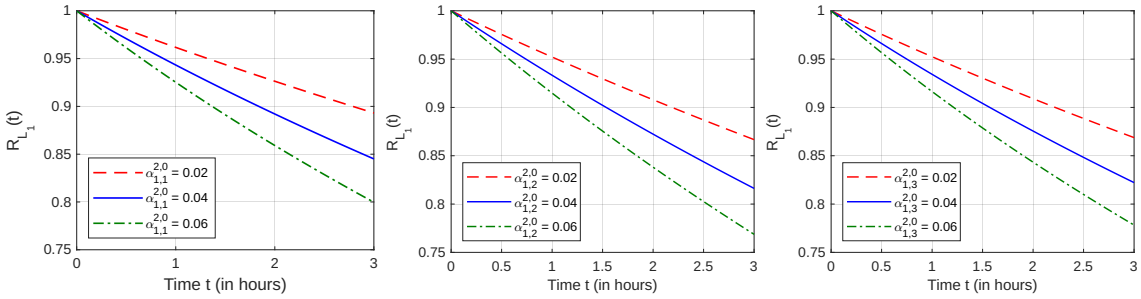

Figure 5: *Effect of failure rates of the components on Reliability(Phase L_1)*

4.1.2 Phase L_2

Phase L_2 initiates immediately after the successful completion of Phase L_1. This phase is longer since the main task of the system is completed during this phase. The initial probability state vector for this Phase is given by $\mathbf{q_1}(3)$. Solving 3 for Phase L_2, the state probabilities vector, $\mathbf{q_2}(t), 3 \leq t \leq 22$, is obtained. The effects of failure rates and repair rates of the components on reliability are observed in Figures 6 and 7.

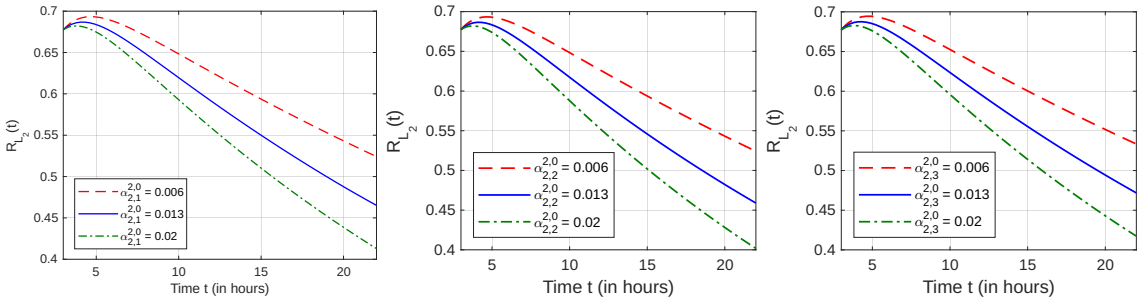

Figure 6: *Effect of failure rates of the components on Reliability(Phase L_2)*

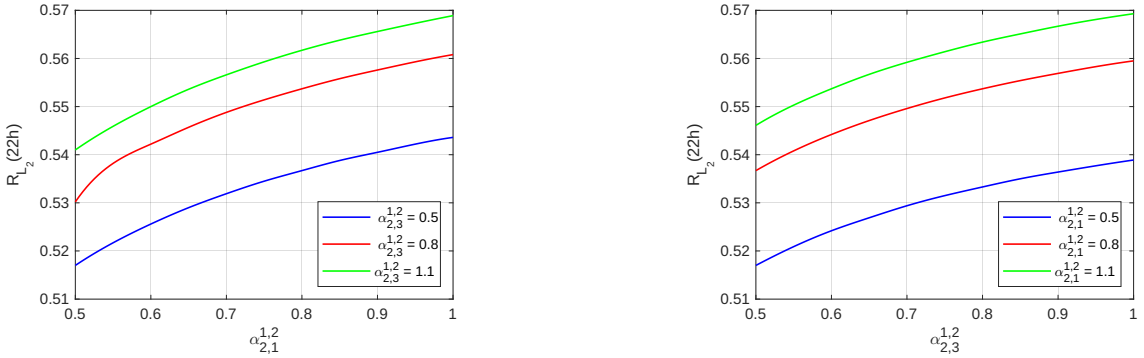

Figure 7: *Effect of repair rates of the components on Reliability(Phase L_2)*

4.1.3 Phase L_3

As soon as Phase L_2 is successfully finished, Phase L_3 begins. The mission's last step is this one. $\mathbf{q_2}(22)$ is the initial probability state vector for this Phase. The state probabilities vector, $\mathbf{q_3}(t), 22 \leq t \leq 24$, is produced by solving 5 for Phase L_3. Figures 8 show how the components of failure rates affect reliability.

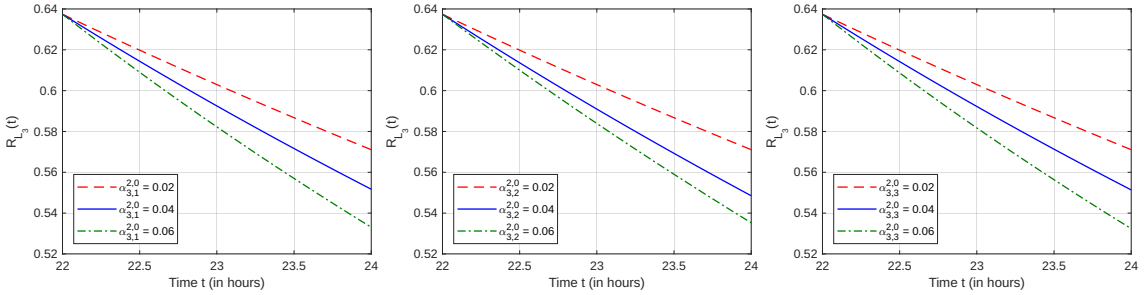

Figure 8: *Effect of failure rates of the components on Reliability(Phase L_1)*

4.1.4 Component Reliability

As the reliability of the tethered HAP system could be measured during each Phase, the reliability of each of the three components can also be analyzed. The graphical analysis of these phases in 12 clearly shows a decreasing trend in component reliability, highlighting the impact of operational duration and stressing the need for proactive maintenance and reliability improvements to ensure mission success.

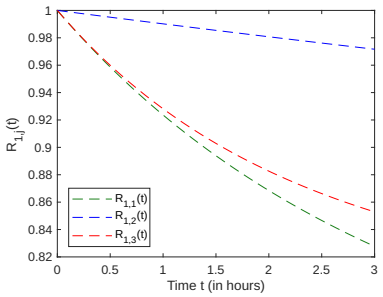

Figure 9: *Phase* L_1

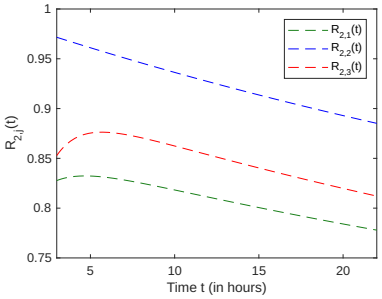

Figure 10: *Phase* L_2

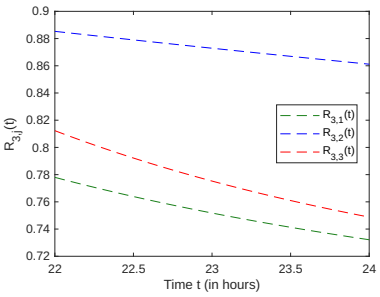

Figure 11: *Phase* L_3

Figure 12: *Reliability of the subsystems during Phase* L_1, L_2 *and* L_3

5. Summary and Possible Extensions

This study conducts an in-depth reliability assessment of a tHAP system, modeled as a PMS. Utilizing a state-spaced Markov model, the analysis considers evolving mission demands and operational conditions across distinct phases. By capturing system breakdowns and state transitions effectively, the model facilitates the evaluation of phase-specific failure probabilities and downtime. Identifying critical phases with elevated risks helps optimize maintenance strategies and redundancy measures, ultimately improving reliability for non-terrestrial applications.

For future research, Monte Carlo simulations will be integrated to enhance probabilistic accuracy. Additionally, a Semi-Markov Process (SMP) approach will be investigated to model phase transitions with arbitrary time distributions, offering a more realistic depiction of mission dynamics. Incorporating real operational data will further refine model parameters, enabling dynamic updates and improved reliability predictions.

References

[1] Vishnevsky, V., Selvamuthu, D., Rykov, V., Kozyrev, D., and Ivanova, N. (2022). Reliability modeling of a flight module of a tethered high-altitude telecommunication platform. In Proceedings of *the 2022 International Conference on Information, Control, and Communication Technologies (ICCT)*, pages 1–6.

[2] Ivanova, N. and Vishnevsky, V. (2021). Application of k-out-of-n: G system and machine learning techniques on reliability analysis of tethered unmanned aerial vehicle. In *International Conference on Information Technologies and Mathematical Modelling*, pages 117–130. Springer.

[3] Ivanova, N. (2020). Modeling and simulation of reliability function of a k-out-of-n: F system. In *International Conference on Distributed Computer and Communication Networks*, pages 271–285. Springer.

[4] Selvamuthu, D., Sivam, A. H., Raj, R., and Vishnevsky, V. (2023). Study of reliability of the on-tether subsystem of a tethered high-altitude unmanned telecommunication platform. *Reliability: Theory & Applications*, 18(1 (72)):172–178.

[5] Xing, L., Shrestha, A., Meshkat, L., and Wang, W. (2009). Incorporating common-cause failures into the modular hierarchical systems analysis. *IEEE Transactions on Reliability*, 58(1):10–19. IEEE.

[6] Xing, L. (2007). Reliability evaluation of phased-mission systems with imperfect fault coverage and common-cause failures. *IEEE Transactions on Reliability*, 56(1):58–68. IEEE.

[7] Xing, L. and Levitin, G. (2013). BDD-based reliability evaluation of phased-mission systems with internal/external common-cause failures. *Reliability Engineering & System Safety*, 112:145–153. Elsevier.

[8] Kozyrev, D. V., Phuong, N. D., Houankpo, H. G. K., and Sokolov, A. (2019). Reliability evaluation of a hexacopter-based flight module of a tethered unmanned high-altitude platform. In *Distributed Computer and Communication Networks*, pages 646–656. Springer International Publishing, Cham.

[9] Perelomov, V. N., Myrova, L. O., Aminev, D. A., and Kozyrev, D. V. (2018). Efficiency enhancement of tethered high altitude communication platforms based on their hardware-software unification. In *Distributed Computer and Communication Networks*, pages 184–200. Springer International Publishing, Cham.

[10] Vishnevsky, V. and Meshcheryakov, R. (2019). Experience of developing a multifunctional tethered high-altitude unmanned platform of long-term operation. In *Interactive Collaborative Robotics: 4th International Conference, ICR 2019, Istanbul, Turkey, August 20–25, 2019, Proceedings 4*, pages 236–244. Springer.

[11] Vishnevsky, V., Tereschenko, B., Tumchenok, D., and Shirvanyan, A. (2017). Optimal method for uplink transfer of power and the design of high-voltage cable for tethered high-altitude unmanned telecommunication platforms. In *Distributed Computer and Communication Networks: 20th International Conference, DCCN 2017, Moscow, Russia, September 25–29, 2017, Proceedings*, pages 240–247. Springer.

[12] Vishnevsky, V. M., Efrosinin, D. V., and Krishnamoorthy, A. (2018). Principles of construction of mobile and stationary tethered high-altitude unmanned telecommunication platforms of long-term operation. In *Distributed Computer and Communication Networks: 21st International Conference, DCCN 2018, Moscow, Russia, September 17–21, 2018, Proceedings 21*, pages 561–569. Springer.

[13] Mittal, N., Ivanova, N., Jain, V., and Vishnevsky, V. (2024). Reliability and availability analysis of high-altitude platform stations through semi-Markov modeling. *Reliability Engineering & System Safety*, 110419. Elsevier.

[14] Belmekki, B. E. Y. and Alouini, M.-S. (2022). Unleashing the potential of networked tethered flying platforms: Prospects, challenges, and applications. *IEEE Open Journal of Vehicular Technology*, 3:278–320. IEEE.

[15] Jain, V., Vishnevsky, V. M., Selvamuthu, D., and Raj, R. (2022). Analysis of power management in a tethered high altitude platform using MAP/PH[3]/1 retrial queueing model. In *International Conference on Distributed Computer and Communication Networks*, pages 218–230. Springer.

[16] Selvamuthu, D., Jain, V., and Raj, R. (2022). Performance analysis for tethered HAP systems: An analytical approach. In *International Conference on Distributed Computer and Communication Networks*, pages 205–217. Springer.

[17] Vishnevsky, V. M., Selvamuthu, D., Rykov, V. V., Kozyrev, D. V., Ivanova, N., and Krishnamoorthy, A. (2024). *Reliability Assessment of Tethered High-Altitude Unmanned Telecommunication Platforms: k-Out-of-n Reliability Models and Applications*. Springer Nature.

[18] Li, X.-Y., Huang, H.-Z., and Li, Y.-F. (2018). Reliability analysis of phased mission system with non-exponential and partially repairable components. *Reliability Engineering & System Safety*, 175:119–127. Elsevier.

[19] Peng, R., Wu, D., Xiao, H., Xing, L., and Gao, K. (2019). Redundancy versus protection for a non-reparable phased-mission system subject to external impacts. *Reliability Engineering & System Safety*, 191:106556. Elsevier.

[20] Tafazoli, M. (2009). A study of on-orbit spacecraft failures. *Acta Astronautica*, 64(2–3):195–205. Elsevier.

[21] Wang, C., Xing, L., Peng, R., and Pan, Z. (2017). Competing failure analysis in phased-mission systems with multiple functional dependence groups. *Reliability Engineering & System Safety*, 164:24–33. Elsevier.

[22] Wu, D., Peng, R., and Xing, L. (2019). Recent advances on reliability of phased mission systems. *Stochastic Models in Reliability, Network Security and System Safety: Essays Dedicated to Professor Jinhua Cao on the Occasion of His 80th Birthday 1*, pages 19–43. Springer.

[23] Li, X.-Y., Xiong, X., Guo, J., Huang, H.-Z., and Li, X. (2022). Reliability assessment of non-repairable multi-state phased mission systems with backup missions. *Reliability Engineering & System Safety*, 223:108462. Elsevier.

[24] Wang, D. and Trivedi, K. S. (2007). Reliability analysis of phased-mission system with independent component repairs. *IEEE Transactions on Reliability*, 56(3):540–551. IEEE.

[25] Wu, B. and Cui, L. (2020). Reliability of repairable multi-state two-phase mission systems with finite number of phase switches. *Applied Mathematical Modelling*, 77:1229–1241. Elsevier.

[26] Mo, Y., Xing, L., and Amari, S. V. (2014). A multiple-valued decision diagram based method for efficient reliability analysis of non-repairable phased-mission systems. *IEEE Transactions on Reliability*, 63(1):320–330. IEEE.